HHS Public Access

Author manuscript

Differentiation. Author manuscript; available in PMC 2017 October 01.

Published in final edited form as:

Differentiation. 2016 ; 92(4): 204–215. doi:10.1016/j.diff.2016.05.006.

Sox9 overexpression in uterine epithelia induces endometrial gland hyperplasia

Gabriel Gonzalez[a], **Shyamin Mehra**[a], **Ying Wang**[a], **Haruhiko Akiyama**[b], and **Richard R. Behringer**[a]

[a]Department of Genetics, University of Texas M.D. Anderson Cancer Center, Houston, TX 77030, USA

[b]Department of Orthopedic Surgery, Gifu University, Gifu City 501-1194, Japan

Abstract

SOX9 is a high mobility group transcription factor that is required in many biological processes, including cartilage differentiation, endoderm progenitor maintenance, hair differentiation, and testis determination. SOX9 has also been linked to colorectal, prostate, and lung cancer. We found that SOX9 is expressed in the epithelium of the adult mouse and human uterus, predominantly marking the uterine glands. To determine if SOX9 plays a role in the development of endometrial cancer we overexpressed Sox9 in the uterine epithelium using a progesterone receptor-Cre mouse model. Sox9 overexpression in the uterine epithelium led to the formation of simple and complex cystic glandular structures in the endometrium of aged-females. Histological analysis revealed that these structures appeared morphologically similar to structures present in patients with endometrial hyperplastic lesions and endometrial polyps that are thought to be precursors of endometrial cancer. The molecular mechanisms that cause the glandular epithelium to become hyperplastic, leading to endometrial cancer are still poorly understood. These findings indicate that chronic overexpression of Sox9 in the uterine epithelium can induce the development of endometrial hyperplastic lesions. Thus, SOX9 expression may be a factor in the formation of endometrial cancer.

Keywords

Sox9; transgenic mouse; uterus; endometrium; cancer

Introduction

In the United States, it is estimated that there were 54,870 women newly diagnosed with endometrial cancer last year, and this malignancy will prove to be fatal for 10,170 (National Cancer Institute). Uterine adenocarcinoma is the most prevalent type of endometrial cancer

Correspondence to: Richard R. Behringer.

arising from uncontrolled growth of the glandular epithelium (GE). Adenocarcinoma development occurs in stages (Silverberg, 2000). The first stage is widely thought to be the manifestation of uterine lesions known as endometrial hyperplasia, sub-classified into simple or complex. In simple hyperplasia, the uterine glands become dilated cysts, showing pseudostratified epithelium, while the stroma appears normal and contains small blood vessels uniformly spaced. In complex hyperplasia the uterine glands show a crowded architecture and are irregular in shape and size often containing numerous side buds, while the stroma appears normal. Various studies have indicated that the presence of cytological atypia, accompanying either simple or complex hyperplasia indicates progression to adenocarcinoma (Silverberg, 2000). In atypical hyperplasia, the uterine gland epithelium loses its normal columnar morphology and the nuclei become rounder. Upon transition to adenocarcinoma, the uterine glands grow in close proximity with minimal stroma between them. One study showed that the progression rate to adenocarcinoma is 4.3% from simple hyperplasia, 16.1% from complex hyperplasia, 7.4% from atypical simple hyperplasia, and 47% from atypical complex hyperplasia (Silverberg, 2000). A study of 7,835 women with endometrial hyperplasia revealed that the cumulative risk of developing adenocarcinoma within 20 years was 4.6% in patients with non-atypical endometrial hyperplasia or disordered proliferative endometrium (Lacey et al., 2010). In contrast, the presence of atypical hyperplasia (simple or complex) raised the cumulative risk of developing adenocarcinoma within 20 years to 27.5%.

Endometrial polyposis is another type of endometrial lesion frequently diagnosed in women (Anastasiadis et al., 2000). Endometrial polyps are described as benign growths that develop in the endometrium. The size of the polyps ranges from a few millimeters up to several centimeters. 20-25% of menopausal and postmenopausal women will develop endometrial polyps (Humphrey et al., 2008). Although mostly benign, endometrial polyps are thought to transform into endometrial cancer (Savelli, 2003). Histological analysis of endometrial polyps usually shows hyperplastic lesions, however, unlike in simple hyperplasia, polyps also display fibrotic stroma and thick-walled blood vessels (Silverberg, 2000). Early discovery and removal is the key factor for treating endometrial polyps before they transform into endometrial cancer.

The molecular events that occur during each stage of endometrial cancer progression are not fully understood. It is thought that the primary driving force that gives rise to the initial hyperplastic lesions is altered estrogen signaling (Bokhman, 1983; Sherman, 2000). Unopposed estrogen potentially exerts a mitogenic signal that can lead to hyperplasia. Later, mutations in KRAS and PTEN are thought to drive the clonal expansion of malignant cells that give rise to adenocarcinomas (Sherman, 2000). Subsequently, it is thought that the malignant cells inactivate the p53 pathway, which regulates cell cycle checkpoints. An understanding of the molecular mechanisms that initiate hyperplasia and subsequently the transformation from benign lesions to cancer will assist with diagnosis and more effective treatment of endometrial cancers.

The main focus of this study was to examine the role of the transcription factor SOX9 during development, tissue homeostasis, and disease. SOX9 is a member of the SRY (sex determination region Y)-related HMG box (SOX) family. The SOX genes are critical in

multiple developmental and physiological processes (Kiefer, 2007). Members of the SOX family contain a conserved high mobility group DNA binding domain. SOX9, SOX8, and SOX10 are transcription factors in the SoxE subgroup that contain an activation domain. Thus, SOX9 primarily acts as a transcriptional activator of target genes. SoxE subgroup genes have been shown to play roles in diverse biological processes, including sex determination, chondrogenesis, and differentiation of Müller glial cells (Foster et al., 1994; Lefebvre and de Crombrugghe, 1998; Poché et al., 2008).

SOX9 is expressed in the epithelium of many organs and has also been linked to colorectal cancer, prostate cancer and lung adenocarcinoma (Darido et al., 2008; Jiang et al., 2010; Wang et al., 2008). SOX9 is activated by fibroblast growth factor (FGF) signaling (Ling et al., 2011) and mutations that result in a constitutively active form of the FGFR2-IIIb have been discovered in 12% of endometrial cancers (Dutt et al., 2008). Moreover, SOX9 expression has been detected in human endometrial cell lines and endometrial tumors (Saegusa et al., 2012). Therefore, we hypothesized that overexpressing SOX9 in the epithelial compartment of the mouse uterus would lead to the development of cancer. To test this idea, we conditionally overexpressed Sox9 in the uterine epithelium and examined these mice for uterine pathologies.

Material and methods

Mice

The Pgr-Cre ($Pgr^{tm2(cre)Lyd}$) mouse strain was obtained from Dr. Franco DeMayo (Baylor College of Medicine, Houston) (Soyal et al., 2005). Sox9-Cre ($Sox9^{tm3(cre)Crm}$) and Sox9 conditional overexpression transgenic mice (CAG-Sox9) were described previously (Akiyama et al., 2005; Kim et al., 2011). R26R-RG (Shioi et al., 2011) mice were obtained from Dr. Go Shioi (RIKEN Center for Developmental Biology, Kobe, Japan). All mice were maintained on a C57BL/6J × 129/SvEv mixed genetic background. Mice were genotyped using tail snips and PCR according to previous reports (Soyal et al., 2005; Akiyama et al., 2005; Kim et al., 2011; Shioi et al., 2011). Estrous cycle status was determined by microscopic examination of vaginal washes (Behringer et al., 2014). All animals were maintained in compliance with the Public Health Service Policy on Humane Care and Use of Laboratory Animals, the U.S. Department of Health and Humane Services Guide for the Care and Use of Laboratory Animals, and the United States Department of Agriculture Animal Welfare Act. All protocols were approved by the University of Texas M.D. Anderson Cancer Center Institutional Animal Care and Use Committee.

Histology

Female reproductive organs were dissected into ice-cold phosphate buffered saline (PBS). The specimens were then fixed in 4% paraformaldehyde (PFA) (Electron Microscopy Sciences, cat# 19208, Hatfield, PA USA) overnight on a nutator at 4°C, dehydrated and embedded in paraffin using standard procedures. The tissues were placed in metal base molds either perpendicular to the bottom for cross-sections or on the side for longitudinal sections. Cross-sections of the uterus were made starting at the most anterior end (oviduct) to the most posterior end (cervix). Hematoxylin and eosin (H&E) staining was performed

using standard procedures. Masson's Trichrome staining was performed using the Accustain Trichrome Stain Kit (Sigma-Aldrich, cat# HT15-1KT, St. Louis, MO USA), following the manufacturer's protocol. Alcian blue staining was performed by placing the tissue sections in a 3% acetic acid solution for 3 minutes. The slides were transferred into 1% Alcian Blue 8GX Stain (Sigma-Aldrich), 3% acetic acid for 30 minutes at room temperature. The slides were then washed in tap water for 10 minutes and rinsed in distilled water. The tissue sections were counterstained with a 0.1% nuclear fast red solution (Sigma-Aldrich) for 5 minutes. The slides were washed in tap water for 1 minute and dehydrated in 95% ethanol. The slides were then transferred into Histo-Clear (National Diagnostics) for 2 minutes three times. Glass cover slips were mounted using Permount (Fisher Scientific).

Immunostaining

Female reproductive organs were dissected and fixed as described above. The next day, the tissues were washed twice for 30 minutes in ice-cold PBS. For frozen sections, the tissues were then transferred into a 15% sucrose solution until they sank to the bottom of the tube. This was repeated using a 30% sucrose solution. The sucrose was discarded and the tissues were embedded and frozen in OCT (Fisher Scientific, cat# 23-730-571, Waltham, MA, USA). Frozen blocks were sectioned using a cryostat. The thickness of the sections varied from 20 μm to 80 μm. The tissue sections were air dried for 5 minutes and then placed in ice-cold acetone for 5 minutes.

For paraffin sections, the tissues were fixed and washed as described above, then processed into paraffin using standard methods and 5 μm sections were cut. Prior to performing immunostaining, the tissue sections were placed in a 55°C oven for 30 min and then deparaffinized and rehydrated. The sections were placed in a 10 mM sodium citrate solution, heated in a microwave oven for 20 minutes, and then cooled to room temperature. The sections were washed with PBS for 5 minutes, and then placed in Hydrogen Peroxide Blocking Reagent (Abcam, ab94666, Cambridge, UK) for 10 minutes.

The slides were transferred into 0.1% Triton X-100 in PBS and for 10 minutes. Blocking solution consisting of 5% sheep serum was added directly on top of each tissue section and incubated for 30 minutes at room temperature. Several primary antibodies used in this study were produced in mice. Therefore, tissue sections were incubated in mouse IgG (M.O.M. ™ Kit, cat# BMK-2202, Vector Laboratories, Burlingame, CA) for 1 hour at room temperature. The primary antibodies, SOX9 (Millipore, AB5535, Billerica, MA, USA, 1:200), E-Cadherin (BD Biosciences, cat# 610181, San Jose, CA, USA, 1:200), p63 (Santa Cruz Biotechnology, sc-25268, Dallas, Texas, USA, 1:100), FOXA2 (Abcam, ab40874, Cambridge, UK, 1:200), Ki67 (Abcam, ab8191, Cambridge, UK, 1:100), Phosphohistone H3 (Millipore, 06-570, Billerica, MA, USA, 1:200), p21(Origene, TA307018, Rockville, MD, USA, 1:200) were diluted in 10% sheep serum and added onto the tissue sections and incubated overnight at 4°C. The next day, the tissue sections were washed 3 times with PBS/0.1% Tween-20 for 10 minutes. For immunofluorescent staining, the sections were then incubated with a 1:400 dilution of the secondary antibody (AlexaFluor, BD Biosciences, San Jose, CA, USA) for 2 hours at room temperature or overnight at 4°C. The tissue sections were washed 3 times with PBS/0.1% Tween-20 for 5 minutes. One drop of Vectashield

mounting medium with DAPI (4′, 6-diamidino-2-phenylindole) (Vector Laboratories, cat# H-1200, Burlingame, CA) was added onto the tissue sections and mounted with a glass coverslip. For immunohistochemical staining, following overnight incubation with primary antibody solution and washing steps, the sections were incubated with 1:500 dilution of the secondary antibody conjugated with horseradish peroxidase for 2 hours at room temperature. The tissue sections were washed 3 times with PBS/0.1% Tween-20 for 5 minutes. The 3, 3′ diaminobenzidine (DAB) chromogen and DAB substrate were mixed together following the manufacturer's protocol (Abcam, ab94665, Cambridge, UK). One drop was added on top of each section and the color was allowed to develop. The slides were washed in tap water for 1 minute and dehydrated in 95% ethanol. The slides were then transferred into Histo-Clear (National Diagnostics, cat# HS-200, Atlanta, GA, USA) for 2 minutes three times. Glass cover slips were mounted using Permount (Fisher Scientific, cat# SP15-100, Waltham, MA, USA).

Image capture and post-acquisition processing

Confocal fluorescent images were obtained using a Nikon C2 Confocal System (Nikon Corporation, Tokyo, Japan) with 405/488/561/640 nm solid-state lasers and inverted eclipse Ti-E microscope with CFI Plan Apochromat Lambda 10x, 20x, and 60x objectives. Z-stacks were captured and a maximum intensity Z-projection was applied to the stacks. Z-stacks were processed using Imaris (Bitplane.com), which allowed us to adjust the color histogram of each color channel and background. In some cases, processed images show a pseudo-colored signal with a light-colored background.

TUNEL analysis

Paraffin sections were deparaffinized and rehydrated for TUNEL analysis, using the In Situ Cell Death Detection Kit, Fluorescein (Sigma-Aldrich, cat# 11684795910, St. Louis, MO USA) according to the manufacturer's instructions. Vectashield mounting medium with DAPI was added to the processed slides that were mounted with a glass coverslip.

H-score analysis of Ki-67 immunostaining

Semi-quantitative analysis was performed using an H-score analysis by two independent observers. The proportion (0-100) and intensity of Ki-67 nuclear immunostaining (0: no staining; 1: weak staining; 2: moderate staining, 3: strong staining) were used to calculate an H-score. A t-test was used to compare potential differences in H-scores between control and experimental samples.

Results

SOX9 is expressed in mouse and human uterine epithelial tissues

SOX9 is expressed in diverse tissues and organs, including the human endometrium and endometrial cancer (Furuyama et al., 2011; Lefebvre and de Crombrugghe, 1998; Poché et al., 2008; Saegusa et al., 2012). To determine if SOX9 was expressed in the adult mouse uterus, we performed immunofluorescent staining for SOX9. Nuclear-localized SOX9 was detected primarily in the glandular epithelium (GE) (Fig. 1A). A few SOX9-positive cells were also found in the luminal epithelium (LE). SOX9 expression was also examined in the

adult human endometrium (Fig. 1B). Similar to the mouse, nuclear-localized SOX9 was detected in the GE of the human endometrium. Nuclear-localized SOX9 was also found in the human LE. Thus, SOX9 is expressed in the GE and a subset of LE in both mice and woman, suggesting that SOX9 may have a conserved role in uterine gland biology.

Uterine cells expressing Sox9 were also visualized using a transgenic fluorescent protein reporter mouse. We took advantage of a R26R-RG mouse line that carries a Cre-dependent conditional allele that can express a histone 2B fusion with monomeric Cherry fluorescent protein (H2B-mCherry or R) and an enhanced green fluorescent protein localized to cell membranes by fusion to a protein domain that confers a GPI linkage (EGFP-GPI or G) (Shioi et al., 2011; Stewart et al., 2009). Thus, cells that expressed Cre activated RG expression, resulting in a red fluorescent nucleus and green plasma membrane. The fluorescent nuclear marker provided single cell resolution. To express these fluorescent proteins in Sox9-expressing cells, we used Sox9-Cre knock-in mice that carry an allele that preserves Sox9 expression but also expresses Cre in a Sox9-specific pattern (Akiyama et al., 2005). R26R-RG mice were bred to Sox9-Cre knock-in mice and their progeny, Sox9-Cre; R26R-RG double heterozygotes, were used to generate fixed frozen sections of adult uteri that were imaged by confocal microscopy for H2B-mCherry fluorescence. The fixation protocol was compatible with H2B-mCherry activity but inactivated GFP, therefore GFP was not used in the current study. Similar to the SOX9 immunofluorescence studies described above, H2B-mCherry was detected in the uterine glands (Fig. 1C, D). In addition, some luminal epithelial cells also expressed H2B-mCherry.

SOX9 has been shown to regulate cell cycle progression in a rat chondrocytic cell line (Panda et al., 2001). The uterine epithelium undergoes rapid changes in cell cycle as it undergoes waves of proliferation and apoptosis during the estrous cycle (Garry et al., 2010; Huang et al., 2012). Thus, we were curious if SOX9 expression in the uterine epithelium would vary during the estrous cycle. Uteri from nulliparous females at four stages of the estrous cycle, proestrus, estrus, metestrus, and diestrus were dissected. Longitudinal uterine sections were examined for SOX9 by immunofluorescence (Fig. 2). Similar to our initial observations, we detected nuclear-localized SOX9 predominantly in the uterine glands but also in cells and subregions of the LE. No overt differences in SOX9 expression were detected in the uterine glands throughout the estrous cycle. In contrast to the uterine glands, the number of SOX9 positive cells appeared to change in the LE during the estrous cycle. There were more SOX9 positive cells found in proestrus, estrus, and metestrus, compared to diestrus. Thus, SOX9 expression in the LE varies during the estrous cycle. In contrast, SOX9 expression in the uterine glands appears to be constant during the different stages of the estrous cycle.

Generation of a mouse model to overexpress Sox9 in the uterine epithelium

Higher SOX9 labeling indices were observed in human atypical hyperplasia and endometrial carcinoma compared to normal uterine tissue (Saegusa et al., 2012), correlating SOX9 expression with malignancy. To experimentally test the idea that Sox9 can act as a cancer-initiating gene, we created a new mouse model to overexpress Sox9 in the uterine epithelium. CAG-Sox9 transgenic mice carry a construct with a CAG promoter for

ubiquitous expression and a loxP-flanked monomeric red fluorescent protein (RFP) gene followed by multiple polyadenylation signals to terminate transcription. This is followed by a Sox9 cDNA and an intraribosomal entry site (IRES) EGFP expression cassette. In the absence of Cre expression the CAG-Sox9 transgene ubiquitously expresses RFP. However, Cre expression will delete the mRFP polyA cassette, leading to Sox9 and EGFP expression. Pgr-cre knock-in mice were used to express Cre in the postnatal uterine epithelium (Soyal et al., 2005). Pgr is expressed in the mouse uterine epithelium starting at approximately postnatal day (P) 14. Pgr is also active in the uterine stroma and myometrium after female mice reach sexual maturity. To activate Sox9 expression throughout the uterine epithelium, CAG-Sox9 mice were bred with Pgr-Cre mice to generate Pgr-Cre/+; CAG-Sox9/+ males. Pgr-Cre/+; CAG-Sox9/+ males were then crossed with homozygous CAG-Sox9/CAG-Sox9 females to generate Pgr-Cre/+; CAG-Sox9/CAG-Sox9 (Sox9-cOE) females for analysis. +/+; CAG-Sox9/CAG-Sox9 females served as controls. Sox9-cOE females were fertile up to 6 months. We did not breed Sox9-cOE females older than 6 months old.

Overexpression of SOX9 in the uterus of prepubescent females

We compared the gross morphological features of uteri dissected from Sox9-cOE and control females at P21, 28 and 35 prior to full sexual maturity. In these prepubescent females, gross examination of the reproductive tracts revealed no obvious morphological differences between Sox9-cOE and controls (data not shown). In addition, no overt histological differences were observed in H&E stained tissue sections from Sox9-OE and control uteri (data not shown). We analyzed SOX9 expression in the uterine epithelium of Sox9-cOE and control females at P21, 28, and 35 by immunofluorescence staining (Fig. 3). At P21, SOX9 immunofluorescence in the LE and GE appeared comparable between Sox9-cOE controls, with SOX9 positive cells present throughout the uterine glands with some SOX9 positive in the luminal epithelium. However, at P28, a few stromal cells appear to ectopically express SOX9 (Fig. 3I, J). This observation was expected because Pgr-Cre becomes active in the stroma as female mice reach sexual maturity. Moreover, at P35, in addition to SOX9 positive cells in the uterine glands, SOX9 positive cells were found throughout the LE (Fig. 3K, L). Thus, in this model, Sox9 overexpression initiates between P28 and P35 that subsequently expands throughout the LE by P35.

Abnormal uterine structures develop in Sox9-cOE mice

Although SOX9 is expressed throughout the LE as early as P35 in Sox9-cOE mice, no gross morphological or histological differences were observed compared to controls. Therefore, we aged these mice to determine if chronic Sox9 expression could alter the uterus. Sox9-cOE and control uteri were examined at 1-, 2-, 4-, 8-, and 12-month-old time points (Fig. 4, Fig. S1). H&E staining of histological sections showed dilated, cystic uterine glands starting at 2-months of age in Sox9-OE mice that persisted and became more severe at later time points (Fig. 4D, Fig. S1). There were numerous severely dilated uterine gland cysts observed along the entire length of the uterus (Fig. 4D, E, F, Fig. S1). The cysts appeared to encroach upon the myometrium. In 12-month-old Sox9-cOE females, uterine glands were cystically dilated and showed crowding and cribriform appearance (Fig. S1K-N). In contrast, in 12-month-old control females, the uterine glands showed normal histological morphology (Fig. S1I, J). The cysts contained large amounts of eosin-positive material, presumably glandular

secretions (Fig. S1K, M, N). In some cases, the Sox9-cOE uterine glands were microscopically dilated (Fig. 4D, F, S1G, H, K-N), comparable to what is seen in human simple endometrial hyperplasia (Silverberg, 2000). In other cases, the uterine glands were more cribriform and crowded (Fig 4J), similar to what is seen in human complex endometrial hyperplasia (Silverberg, 2000). In a few cases, we observed loss of normal columnar morphology and nuclei that appeared rounder (Fig. S1L, N) similar to cases of atypical hyperplasia. These findings suggest that overexpressing Sox9 in the mouse uterine epithelium leads to the appearance of histopathological findings similar to cases of human endometrial hyperplasia.

The stroma of Sox9-OE female uteri developed fibrosis as early as 2 months of age and this persisted and appeared to become more severe at 4- and 8-months of age (Fig. 4D, J, Fig. S1). At 4 months of age, Mason's Trichrome staining in Sox9-cOE uteri revealed strong staining in the stromal region, indicating increased connective tissue/collagen fibers compared to controls (Fig. 4H, I, K, L). Thus, chronic overexpression of Sox9 appears to influence epithelial organization and stromal differentiation.

In this study, Sox9-cOE and control were aged up to 1 year. Gross examination of the uteri from 1-year-old females revealed gross morphological differences between Sox9-cOE and control uteri (Fig. 5). Under the dissecting microscope, numerous cystoid structures inside the uteri of 1-year-old Sox9-cOE females were observed (Fig. 5D-F). In control females, only 1 or 2 cystic structures were found along the entire length of both uterine horns (Fig. 5A-C). In comparison with controls, the uteri of Sox9-cOE females were filled with cystic structures of variable sizes. A longitudinal incision along the length of the uterus, providing a luminal view, showed that the cystic structures were filled with a white substance (Fig. 5F).

Cellular behaviors in endometrial hyperplastic lesions in Sox9-cOE mice

To determine if the endometrial hyperplastic lesions of Sox9-cOE females are formed by increased cell proliferation of the GE, immunofluorescent staining for markers of cell proliferation was performed. The mouse uterine epithelium undergoes rapid changes between cell proliferation and apoptosis, depending on the stage of the estrous cycle (Garry et al., 2010; Huang et al., 2012). To minimize potential differences in cell proliferation that are typically dependent on estrous cycle stage, estrous cycle status for each female was determined prior to sacrifice. Uteri were examined from 2- to 4-month-old females. The number of cells undergoing mitosis was assessed by staining for phosphohistone H3 (PH3). No differences in the numbers of PH3 positive cells between Sox9-cOE and controls were detected (Fig. 6A, D). Tissue sections were also stained for Ki-67, a marker of cell proliferation. No major differences in Ki-67 immunostaining were observed in uterine tissue sections between estrous stage-matched Sox9-cOE and controls (Fig. 6B, E). Both groups displayed Ki-67 positive staining in the LE during estrus, whereas during diestrus, the number of Ki-67 positive cells was negligible (data not shown). In the uterine glands, low numbers of Ki-67 positive cells were detected during estrus and diestrus. Therefore, there were no overt changes in cell proliferation detected between Sox9-cOE and controls females at 2 and 4-months of age. To determine if there were changes in the number of cells

undergoing apoptosis during metestrus, we performed TUNEL staining. No differences in the numbers of TUNEL positive cells between Sox9-cOE and controls were detected (Fig. 6C, F).

Aged Sox9-cOE females showed greater number of uterine glands that appeared cystically dilated and showed crowding and cribriform appearance. Therefore, Ki-67 immunostaining was performed in uterine sections of control and Sox9-cOE mice 8- and 12-months of age (Fig. 7A, B). Control tissues contained few Ki-67 positive GE cells (Fig. 7C, D). Compared to controls, Sox9-cOE uteri contained areas with high numbers of Ki-67 positive GE cells (Fig. 7E) and adjacent areas with few Ki-67 positive GE cells (Fig. 7F). An H-score was used to evaluate the proportion and intensity of Ki-67 immunostaining and a t-test was used to compare potential differences between the groups (Fig. 7G). A slight difference, although not statistically different, was noticed between Sox9-cOE and controls females examined at 8- and 12-months of age (Fig. 7, data not shown). We did not observe a correlation between Ki-67 staining and morphology.

Differentiation status of endometrial hyperplastic lesions in Sox9-cOE mice

The differentiation status of the Sox9-cOE uterine tissues was examined by molecular marker analysis. FOXA2 is a winged helix transcription factor that is expressed in mouse uterine glands but not the LE (Jeong et al., 2010). FOXA2 was expressed in the uterine glands of 8-month-old controls and some cells of the cystically-dilated hyperplastic uterine glands of Sox9-cOE females (Fig. 8A, B). This suggests that even though the Sox9-cOE uterine glands show structural abnormalities, they retain uterine gland identity, at least for FOXA2.

TP63 (tumor protein p63) is a transcription factor expressed in stratified epithelium but not in columnar epithelium (Kurita et al., 2005). Conditionally inactivating Wnt4 in uterine glands led to abnormal glandular differentiation and appearance of a p63-expressing basal epithelial layer in mouse uterine glands (Franco et al., 2011). SOX9 and WNT4 play opposing roles during gonadal differentiation (Uhlenhaut et al., 2009). Therefore, we examined the differentiation state of the uterine epithelium in Sox9-cOE mice by performing immunofluorescent staining for p63 and SOX9 (Fig. 8C-F). As a control, we included tissue sections with cervix, which possesses a stratified epithelium. The cervical epithelium stained positively for p63 (Fig. 8E, F). However, p63 immunostaining was not detected in the uterine glands or luminal epithelium of Sox9-cOE and controls at 2-, 4-, 8-months of age, and also in 1-year-old tissue sections that display epithelial hyperplasia (Fig. 8C, D). This indicates that SOX9 does not appear to influence the expression of Tp63 in the mouse GE.

Discussion

SOX9 marks uterine glands

The uterus is an organ that undergoes coordinated cyclic waves of cell death followed by rapid tissue regeneration by proliferation and differentiation (Gray et al., 2001; Medh and Thompson, 2000). During menstruation the stratum functionalis is shed and then regenerated. It has been proposed that glandular epithelial cells within the stratum basalis

form the new stratum functionalis (Spencer et al., 2005). Specifically, adult stem cells within the stratum basalis, are thought to support the rapid regeneration of the stratum functionalis (Gargett, 2007). Cre-based lineage-tracing experiments in the mouse suggest that Sox9-expressing cells can differentiate into various cell types in the intestine, liver and pancreas (Furuyama et al., 2011). This suggests that Sox9-expressing cells may function as epithelial progenitor cells in these organs. In human endometrial samples, it was shown that SOX9 was expressed in the deeper stratum basalis region, the area retained after the stratum functionalis is shed during menstruation (Valentijn et al., 2013). Cells expressing SOX9 also showed a pattern of expression similar to that of SSEA-1, a marker of pluripotent cells, and were found to express high telomerase activity and had longer telomeres (Valentijn et al., 2013). Here, we show that nuclear-localized SOX9 is expressed in the uterine epithelium in both mouse and human. SOX9 expression was predominantly found throughout the uterine glands. In sections of the human endometrium, a similar expression pattern was observed by the Human Protein Atlas (Uhlen et al., 2010). In addition, other studies have shown that SOX9 is expressed in human endometrial glands (Saegusa et al., 2012; Valentijn et al., 2013). Therefore, there is ample evidence demonstrating that SOX9 is expressed in the glandular epithelium of the uterus, in both human and mice.

In our Sox9-RG female mice, the uterine glands expressed mCherry fluorescent protein, suggesting that the GE was expressing Sox9 or was derived from cells that had expressed Sox9 at one point. It was previously shown that the GE retains BrdU for longer periods than the LE, suggesting that the GE harbors uterine epithelial progenitor cells (Kaitu'u-Lino et al., 2010). We observed that SOX9 was expressed in the GE throughout the estrous cycle of mice but SOX9 expression varied in the LE, depending on estrous cycle stage. In humans, SOX9 expression varies during the menstrual cycle, becoming elevated during the proliferative phase compared to the secretory phase (Saegusa et al., 2012). It is possible that SOX9-expressing progenitor epithelial cells divide during the proliferative stage and migrate towards the luminal surface. There, they either undergo apoptosis or perhaps incorporate into the luminal epithelium. A minority of the LE cells in the uterus of Sox9-RG mice were mCherry positive, suggesting that there may also be a resident pool of progenitor cells for the luminal epithelium.

Overexpression of Sox9 in the uterine epithelium leads to endometrial hyperplasia

We have shown that SOX9 is expressed in uterine glands in mouse and human, suggesting that it regulates processes in the uterine GE. We generated a new mouse model to overexpress Sox9 in the female reproductive tract. We used the Pgr promoter, driving Cre expression to activate Sox9 expression in the uterine epithelium, stroma and myometrium (Soyal et al., 2005). Previously, Kim et al., (2011) showed that the CAG-Sox9 transgene, when activated by Sox9-Cre, was expressed at ~1.5X the levels of endogenous Sox9 in neonatal rib cartilage and that the downstream chondrocyte markers Aggregan and Col2a1 were up-regulated to similar levels. We speculate that similar levels of Sox9 were achieved in the Sox9-cOE uterine glands, whereas the fold increase in the luminal epithelium may be much higher because SOX9 is predominantly expressed in uterine glands. We found that before puberty, the uteri of Sox9-cOE females appeared morphologically and histologically similar to control littermates, even though SOX9 was detected in the entire uterine

epithelium by P35. Therefore, overexpressing Sox9 in the uterine epithelium does not result in immediate morphological abnormalities. However, the endometrium showed a progression to hyperplasia starting at 2-months of age, indicating that the cystically dilated uterine gland lesions developed after the females became sexually mature. Perhaps the continuous remodeling of the uterine tissues during repeated estrous cycles facilitates Sox9-induced abnormalities. The Pgr-Cre allele also expresses in postnatal stroma (Soyal et al., 2005). We did detect some SOX9-expressing cells in the uterine stroma from at least P21 to P35. It is possible that ectopic expression of SOX9 in the uterine stroma also contributed to the subsequent glandular hyperplasia.

These abnormal uterine glands in our mouse model resembled human endometrial polyps (Anastasiadis et al., 2000; Deligdisch et al., 2000). Histologically, these structures appeared as cystically dilated uterine glands present in the endometrium surrounded by fibrotic stroma that could invade the myometrium (adenomyosis). In contrast to human endometrial polyps, the abnormal uterine glands in our mouse model did not grow into the uterine cavity (Deligdisch et al., 2000). 20-25% of women over the age of 40 will eventually develop endometrial polyps (Humphrey et al., 2008). Endometrial polyps are usually benign, although it is thought that they can transform into endometrial cancer (Savelli, 2003). Treating mice that contain only one functional p53 allele (p53 +/-) with N-ethyl-N-nitrosourea (ENU), a potent mutagen, led to the development of endometrial polyps with a similar histology to those observed in our mouse model (Mitsumori et al., 2000). These ENU-treated mice also developed endometrial stromal sarcomas that contained point mutations in the remaining p53 allele. Our data suggest that the Sox9-induced uterine gland abnormalities in our mouse model may be preneoplastic lesions for endometrial cancer.

The oldest Sox9-cOE uteri also showed complex hyperplasia; glands that varied in size and contained numerous buds. The uterine glands showed a crowded cytoarchitecture, although stroma was observed between the epithelium, indicating that although hyperplastic, the lesions had not progressed to endometrial adenocarcinoma. Therefore, Sox9-cOE females develop cellular changes that are considered hallmarks of disease progression. The cytological abnormalities resembled what is seen in human simple endometrial hyperplasia (Deligdisch et al., 2000; Silverberg, 2000). Moreover, Sox9-cOE females developed uterine glands that grew in a more cribriform, crowded fashion, similar to what is seen in human complex endometrial hyperplasia (Silverberg, 2000). Endometrial polyps and endometrial hyperplastic lesions are thought to develop into endometrioid adenocarcinoma (Savelli, 2003). Thus, the polypoid-like lesions observed in Sox9-cOE uteri may be progressing to a disease state comparable to that found in humans.

Cellular mechanisms of uterine gland hypertrophy in Sox9-cOE mice

The hyperplastic lesions that develop in Sox9-cOE females may be the result of abnormal cell proliferation. SOX9 is expressed primarily in the GE, which has a lower proliferation rate compared to the LE (Kaitu'u-Lino et al., 2010). In adult females of reproductive age, there was no statistical difference in GE cell proliferation between Sox9-cOE and controls. Similarly, there was no statistical difference for Ki-67 immunostaining assessed by H-score analysis in females (> 8-months of age) past their reproductive age. However, Sox9-cOE

uteri contained focal areas with high number of Ki-67 positive GE cells. Therefore, focal hypertrophy in females past reproductive age may explain the appearance of the large number of cysts observed by gross morphology in uteri of mice 8-months-old and older. Our studies are consistent with the idea that Sox9 must be tightly regulated to maintain uterine gland homeostasis.

In summary, our findings demonstrate that overexpression of Sox9 is sufficient to induce changes to the tissue architecture of the female mouse reproductive tract and plays a role in the development of histological lesions that resemble human endometrial polyps and hyperplasia. This implicates SOX9 in the pathogenesis of these endometrial diseases and may contribute to the formation of endometrial cancer.

Supplementary Material

Refer to Web version on PubMed Central for supplementary material.

Acknowledgments

We thank Dr. Russell Broaddus (M.D. Anderson Cancer Center) for providing human uterine tissues, Dr. Franco DeMayo (Baylor College of Medicine) for providing the Pgr-Cre mouse strain, and David Stewart for strain rederivation. Supported by National Institutes of Health (NIH) grant HD030284 and the Ben F. Love Endowment to R.R.B. G.G. was supported by National Cancer Institute T32 grant CA09299. Veterinary resources were supported by NIH grant CA16672.

References

Akiyama H, Kim JE, Nakashima K, Balmes G, Iwai N, Deng JM, Zhang Z, Martin JF, Behringer RR, Nakamura T, de Crombrugghe B. Osteo-chondroprogenitor cells are derived from Sox9 expressing precursors. Proc Natl Acad Sci U S A. 2005; 102:14665–14670. DOI: 10.1073/pnas.0504750102 [PubMed: 16203988]

Anastasiadis PG, Koutlaki NG, Skaphida PG, Galazios GC, Tsikouras PN, Liberis VA. Endometrial polyps: prevalence, detection, and malignant potential in women with abnormal uterine bleeding. Eur J Gynaecol Oncol. 2000; 21:180–183. [PubMed: 10843481]

Behringer, R.; Gertsenstein, M.; Vintersten Nagy, K.; Nagy, A. Manipulating the Mouse Embryo: A Laboratory Manual. Fourth Edi. Cold Spring Harbor Laboratory Press; 2014.

Bokhman JV. Two pathogenetic types of endometrial carcinoma. Gynecol Oncol. 1983; 15:10–17. [PubMed: 6822361]

Darido C, Buchert M, Pannequin J, Bastide P, Zalzali H, Mantamadiotis T, Bourgaux JF, Garambois V, Jay P, Blache P, Joubert D, Hollande F. Defective claudin-7 regulation by Tcf-4 and Sox-9 disrupts the polarity and increases the tumorigenicity of colorectal cancer cells. Cancer Res. 2008; 68:4258–4268. DOI: 10.1158/0008-5472.CAN-07-5805 [PubMed: 18519685]

Deligdisch L, Kalir T, Cohen CJ, de Latour M, Le Bouedec G, Penault-Llorca F. Endometrial histopathology in 700 patients treated with tamoxifen for breast cancer. Gynecol Oncol. 2000; 78:181–6. DOI: 10.1006/gyno.2000.5859 [PubMed: 10926800]

Dutt A, Salvesen HB, Chen TH, Ramos AH, Onofrio RC, Hatton C, Nicoletti R, Winckler W, Grewal R, Hanna M, Wyhs N, Ziaugra L, Richter DJ, Trovik J, Engelsen IB, Stefansson IM, Fennell T, Cibulskis K, Zody MC, Akslen La, Gabriel S, Wong KK, Sellers WR, Meyerson M, Greulich H. Drug-sensitive FGFR2 mutations in endometrial carcinoma. Proc Natl Acad Sci U S A. 2008; 105:8713–8717. DOI: 10.1073/pnas.0803379105 [PubMed: 18552176]

Foster JW, Dominguez-Steglich MA, Guioli S, Kwok C, Weller PA, Stevanovic M, Weissenbach J, Mansour S, Young ID, Goodfellow PN, Brook JD, Schafer AJ. Campomelic dysplasia and autosomal sex reversal caused by mutations in an SRY-related gene. Nature. 1994; 372:525–530. [PubMed: 7990924]

Franco HL, Dai D, Lee KY, Rubel Ca, Roop D, Boerboom D, Jeong JW, Lydon JP, Bagchi IC, Bagchi MK, DeMayo FJ. WNT4 is a key regulator of normal postnatal uterine development and progesterone signaling during embryo implantation and decidualization in the mouse. FASEB J. 2011; 25:1176–1187. DOI: 10.1096/fj.10-175349 [PubMed: 21163860]

Furuyama K, Kawaguchi Y, Akiyama H, Horiguchi M, Kodama S, Kuhara T, Hosokawa S, Elbahrawy A, Soeda T, Koizumi M, Masui T, Kawaguchi M, Takaori K, Doi R, Nishi E, Kakinoki R, Deng JM, Behringer RR, Nakamura T, Uemoto S. Continuous cell supply from a Sox9-expressing progenitor zone in adult liver, exocrine pancreas and intestine. Nat Genet. 2011; 43:34–41. DOI: 10.1038/ng.722 [PubMed: 21113154]

Gargett CE. Uterine stem cells: What is the evidence? Hum Reprod Updat. 2007; 13:87–101. DOI: 10.1093/humupd/dml045

Garry R, Hart R, Karthigasu Ka, Burke C. Structural changes in endometrial basal glands during menstruation. BJOG. 2010; 117:1175–85. DOI: 10.1111/j.1471-0528.2010.02630.x [PubMed: 20560946]

Gray CA, Bartol FF, Tarleton BJ, Wiley AA, Johnson GA, Bazer FW, Spencer TE, Al GET. Developmental Biology of Uterine Glands. Biol Reprod. 2001; 65:1311–1323. DOI: 10.1095/biolreprod65.5.1311 [PubMed: 11673245]

Huang CC, Orvis GD, Wang Y, Behringer RR. Stromal-to-epithelial transition during postpartum endometrial regeneration. PLoS One. 2012; 7:e44285.doi: 10.1371/journal.pone.0044285 [PubMed: 22970108]

Humphrey, PA.; Dehner, LP.; Pfeifer, JD. The Washington Manual of Surgical Pathology. 1. Lippincott Williams & Wilkins; 2008.

Jeong JW, Kwak I, Lee KY, Kim TH, Large MJ, Stewart CL, Kaestner KH, Lydon JP, DeMayo FJ. Foxa2 is essential for mouse endometrial gland development and fertility. Biol Reprod. 2010; 83:396–403. DOI: 10.1095/biolreprod.109.083154 [PubMed: 20484741]

Jiang SS, Fang WT, Hou YH, Huang SF, Yen BL, Chang JL, Li SM, Liu HP, Liu YL, Huang CT, Li YW, Jang TH, Chan SH, Yang SJ, Hsiung Ca, Wu CW, Wang LH, Chang IS. Upregulation of SOX9 in lung adenocarcinoma and its involvement in the regulation of cell growth and tumorigenicity. Clin Cancer Res. 2010; 16:4363–4373. DOI: 10.1158/1078-0432.CCR-10-0138 [PubMed: 20651055]

Kaitu'u-Lino TJ, Ye L, Gargett CE. Reepithelialization of the uterine surface arises from endometrial glands: evidence from a functional mouse model of breakdown and repair. Endocrinology. 2010; 151:3386–3395. DOI: 10.1210/en.2009-1334 [PubMed: 20444944]

Kiefer JC. Back to basics: Sox genes. Dev Dyn. 2007; 236:2356–2366. DOI: 10.1002/dvdy.21218 [PubMed: 17584862]

Kim Y, Murao H, Yamamoto K, Deng JM, Behringer RR, Nakamura T, Akiyama H. Generation of transgenic mice for conditional overexpression of Sox9. J Bone Miner Metab. 2011; 29:123–129. DOI: 10.1007/s00774-010-0206-z [PubMed: 20676705]

Kurita T, Cunha GR, Robboy SJ, Mills Aa, Medina RT. Differential expression of p63 isoforms in female reproductive organs. Mech Dev. 2005; 122:1043–55. DOI: 10.1016/j.mod.2005.04.008 [PubMed: 15922574]

Lacey JV, Sherman ME, Rush BB, Ronnett BM, Ioffe OB, Duggan Ma, Glass AG, Richesson Da, Chatterjee N, Langholz B. Absolute risk of endometrial carcinoma during 20-year follow-up among women with endometrial hyperplasia. J Clin Oncol. 2010; 28:788–792. DOI: 10.1200/JCO.2009.24.1315 [PubMed: 20065186]

Lefebvre V, de Crombrugghe B. Toward understanding S0X9 function in chondrocyte differentiation. Matrix Biol. 1998; 16:529–540. [PubMed: 9569122]

Ling S, Chang X, Schultz L, Lee TK, Chaux A, Marchionni L, Netto GJ, Sidransky D, Berman DM. An EGFR-ERK-SOX9 signaling cascade links urothelial development and regeneration to cancer. Cancer Res. 2011; 71:3812–3821. DOI: 10.1158/0008-5472.CAN-10-3072 [PubMed: 21512138]

Medh R, Thompson B. Hormonal regulation of physiological cell turnover and apoptosis. Cell Tissue Res. 2000; 301:101–124. [PubMed: 10928284]

Mitsumori K, Onodera H, Shimo T, Yasuhara K, Takagi H, Koujitani T, Hirose M, Maruyama C, Wakana S. Rapid induction of uterine tumors with p53 point mutations in heterozygous p53-

deficient CBA mice given a single intraperitoneal administration of N-ethyl-N-nitrosourea. Carcinogenesis. 2000; 21:1039–1042. [PubMed: 10783330]

Panda DK, Miao D, Lefebvre V, Hendy GN, Goltzman D. The Transcription Factor SOX9 Regulates Cell Cycle and Differentiation Genes in Chondrocytic CFK2 Cells. J Biol Chem. 2001; 276:41229–41236. DOI: 10.1074/jbc.M104231200 [PubMed: 11514554]

Poché RA, Furuta Y, Chaboissier MC, Schedl A, Behringer RR. Sox9 is expressed in mouse multipotent retinal progenitor cells and functions in Müller Glial cell development. J Comp Neurol. 2008; 510:237–250. [PubMed: 18626943]

Saegusa M, Hashimura M, Suzuki E, Yoshida T, Kuwata T. Transcriptional upregulation of Sox9 by NF-κB in endometrial carcinoma cells, modulating cell proliferation through alteration in the p14(ARF)/p53/p21(WAF1) pathway. Am J Pathol. 2012; 181:684–92. DOI: 10.1016/j.ajpath.2012.05.008 [PubMed: 22698986]

Savelli L. Histopathologic features and risk factors for benignity, hyperplasia, and cancer in endometrial polyps. Am J Obstet Gynecol. 2003; 188:927–931. DOI: 10.1067/mob.2003.247 [PubMed: 12712087]

Sherman ME. Theories of endometrial carcinogenesis: a multidisciplinary approach. Mod Pathol. 2000; 13:295–308. DOI: 10.1038/modpathol.3880051 [PubMed: 10757340]

Shioi G, Kiyonari H, Abe T, Nakao K, Fujimori T, Jang CW, Huang CC, Akiyama H, Behringer RR, Aizawa S. A mouse reporter line to conditionally mark nuclei and cell membranes for in vivo live-imaging. Genesis. 2011; 49:570–578. DOI: 10.1002/dvg.20758 [PubMed: 21504045]

Silverberg SG. Problems in the differential diagnosis of endometrial hyperplasia and carcinoma. Mod Pathol. 2000; 13:309–327. DOI: 10.1038/modpathol.3880053 [PubMed: 10757341]

Soyal SM, Mukherjee A, Lee KYS, Li J, Li H, DeMayo FJ, Lydon JP. Cre-mediated recombination in cell lineages that express the progesterone receptor. genesis. 2005; 41:58–66. [PubMed: 15682389]

Spencer TE, Hayashi K, Hu J, Carpenter KD. Comparative developmental biology of the mammalian uterus. Curr Top Dev Biol. 2005; 68:85–122. DOI: 10.1016/S0070-2153(05)68004-0 [PubMed: 16124997]

Stewart MD, Jang C, Hong NW, Austin AP, Behringer RR. Dual fluorescent protein reporters for studying cell behaviors in vivo. Genesis. 2009; 47:708–717. DOI: 10.1002/dvg.20565.Dual [PubMed: 19813259]

Uhlen M, Oksvold P, Fagerberg L, Lundberg E, Jonasson K, Forsberg M, Zwahlen M, Kampf C, Wester K, Hober S, Wernerus H, Bjorling L, Ponten F. Towards a knowledge-based Human Protein Atlas. Nat Biotech. 2010; 28:1248–1250.

Uhlenhaut NH, Jakob S, Anlag K, Eisenberger T, Sekido R, Kress J, Treier AC, Klugmann C, Klasen C, Holter NI, Riethmacher D, Schütz G, Cooney AJ, Lovell-Badge R, Treier M. Somatic sex reprogramming of adult ovaries to testes by FOXL2 ablation. Cell. 2009; 139:1130–42. DOI: 10.1016/j.cell.2009.11.021 [PubMed: 20005806]

Valentijn AJ, Palial K, Al-Lamee H, Tempest N, Drury J, Von Zglinicki T, Saretzki G, Murray P, Gargett CE, Hapangama DK. SSEA-1 isolates human endometrial basal glandular epithelial cells: phenotypic and functional characterization and implications in the pathogenesis of endometriosis. Hum Reprod. 2013; 28:2695–2708. DOI: 10.1093/humrep/det285 [PubMed: 23847113]

Wang H, Leav I, Ibaragi S, Wegner M, Hu G, Lu ML, Balk SP, Yuan X. SOX9 is expressed in human fetal prostate epithelium and enhances prostate cancer invasion. Cancer Res. 2008; 68:1625–1630. DOI: 10.1158/0008-5472.CAN-07-5915 [PubMed: 18339840]

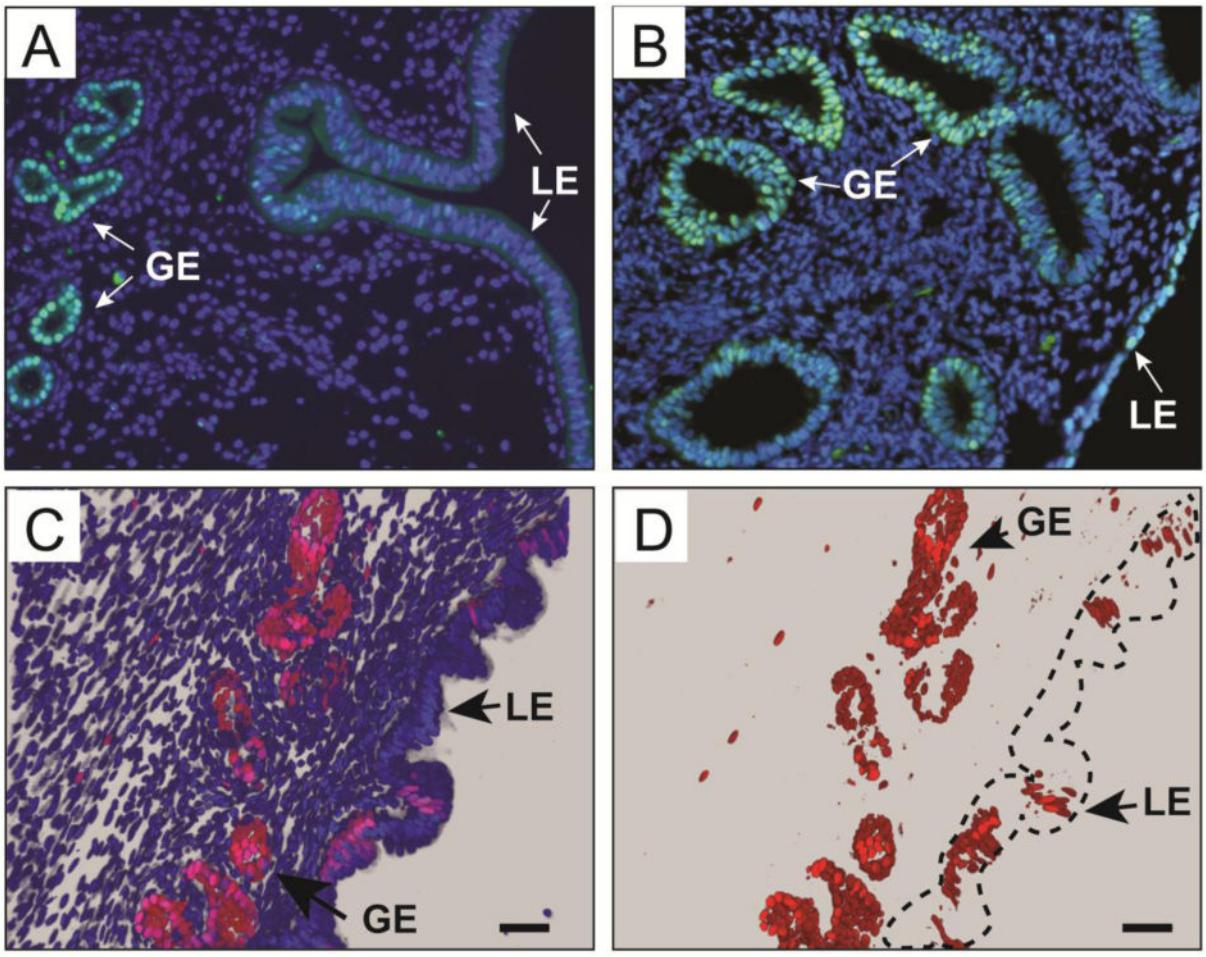

Fig. 1.

SOX9 expression in the adult mouse and human uterus. (A, B) Immunofluorescent staining using an α-SOX9 antibody (green) counterstained with DAPI (blue) of proestrus stage adult mouse (A) and postmenopausal human (B) uterine sections. (C, D) Fluorescent images of 8-week-old Sox9-Cre; R26R-RG double heterozygous female, showing H2BmCherry-positive cells (red) present mostly in the GE. (C) Nuclei were counterstained with DAPI (blue). (D) The blue channel (DAPI) was removed to show that most H2BmCherry-positive nuclei are present in the GE. Dotted line outlines the luminal epithelium. GE, glandular epithelium; LE, luminal epithelium. Scale bars, 50 μm.

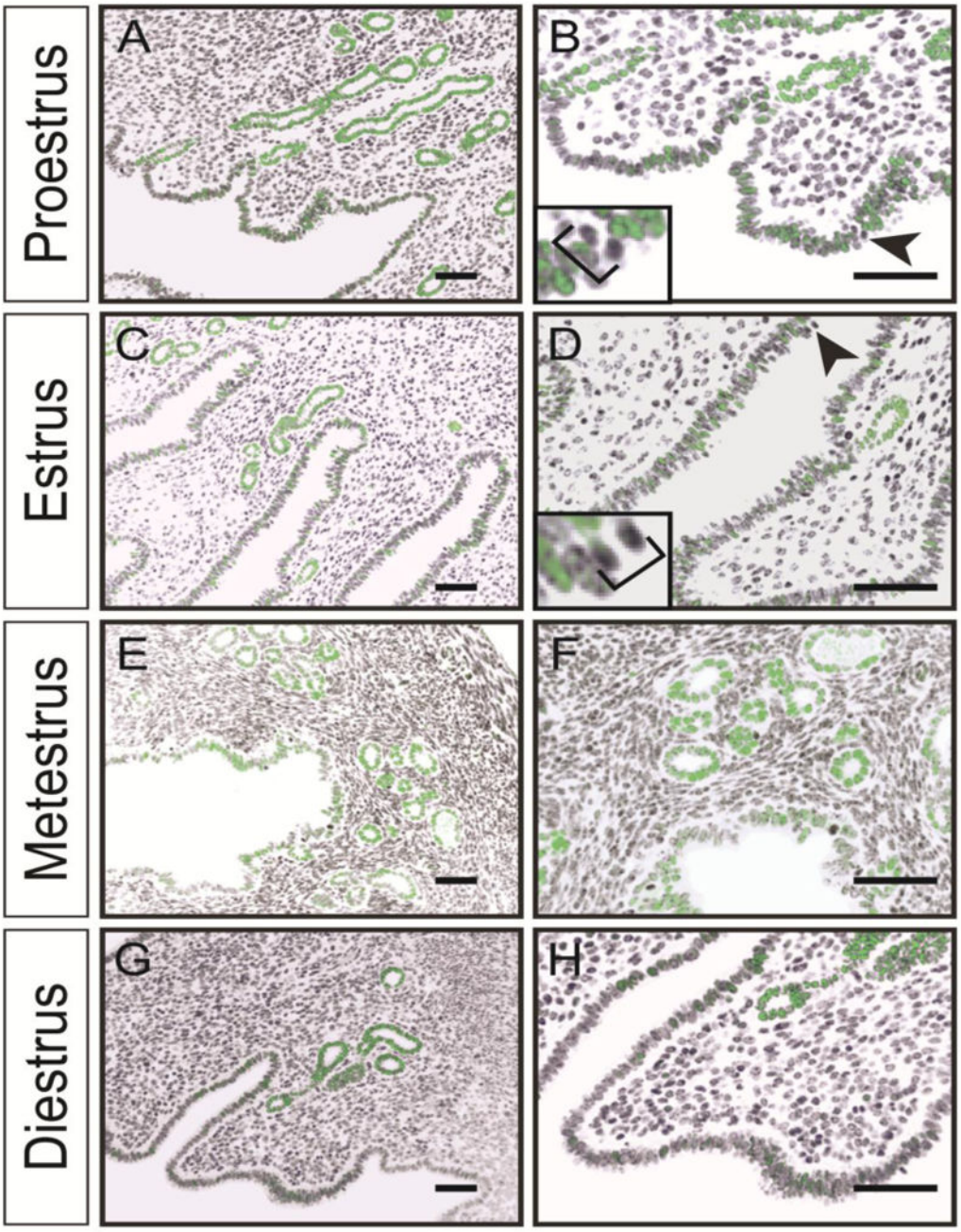

Fig. 2.

SOX9 expression during the estrous cycle. (A, C, E, G) Immunofluorescent staining using an α-SOX9 antibody (green) counterstained with DAPI (black) of adult uterine sections. (B, D, F, H) higher magnifications of A, C, E, G, respectively. Note that most mitotic figures in B and D (black arrowheads and insets) are devoid of SOX9. Scale bar, 50 μm

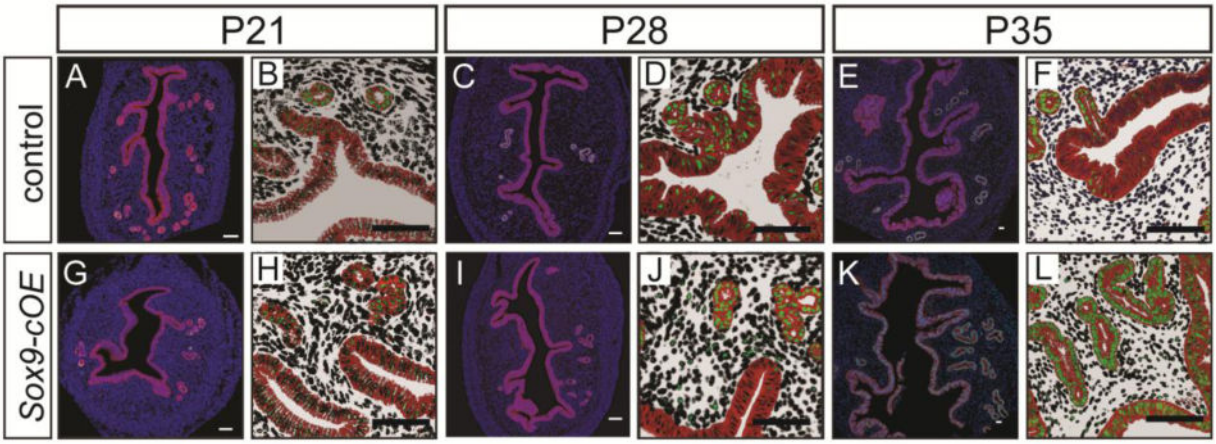

Fig. 3.

Wild-type and SOX9 overexpression in the uteri of prepubertal female mice. (A-L) Immunofluorescent staining for SOX9 (green) and E-cadherin (red) at P21, 28, and 35. Uteri from control (A-F) and Sox9-cOE (G-L) females. (B, D, F, H, J, L) Higher magnification views of A, C, E, G, I, K, respectively, with the background subtracted to emphasize SOX9. (A-F) SOX9 overexpression is observed in the LE and GE of uteri from Sox9-cOE at P35 (K, L) compared to controls (E, F). Some SOX9 was also detected in the stroma and myometrium of uteri from Sox9-cOE at P28 (I, J) and P35 (K, L) compared to controls (C-F). DAPI, blue. Scale bar, 50 μm.

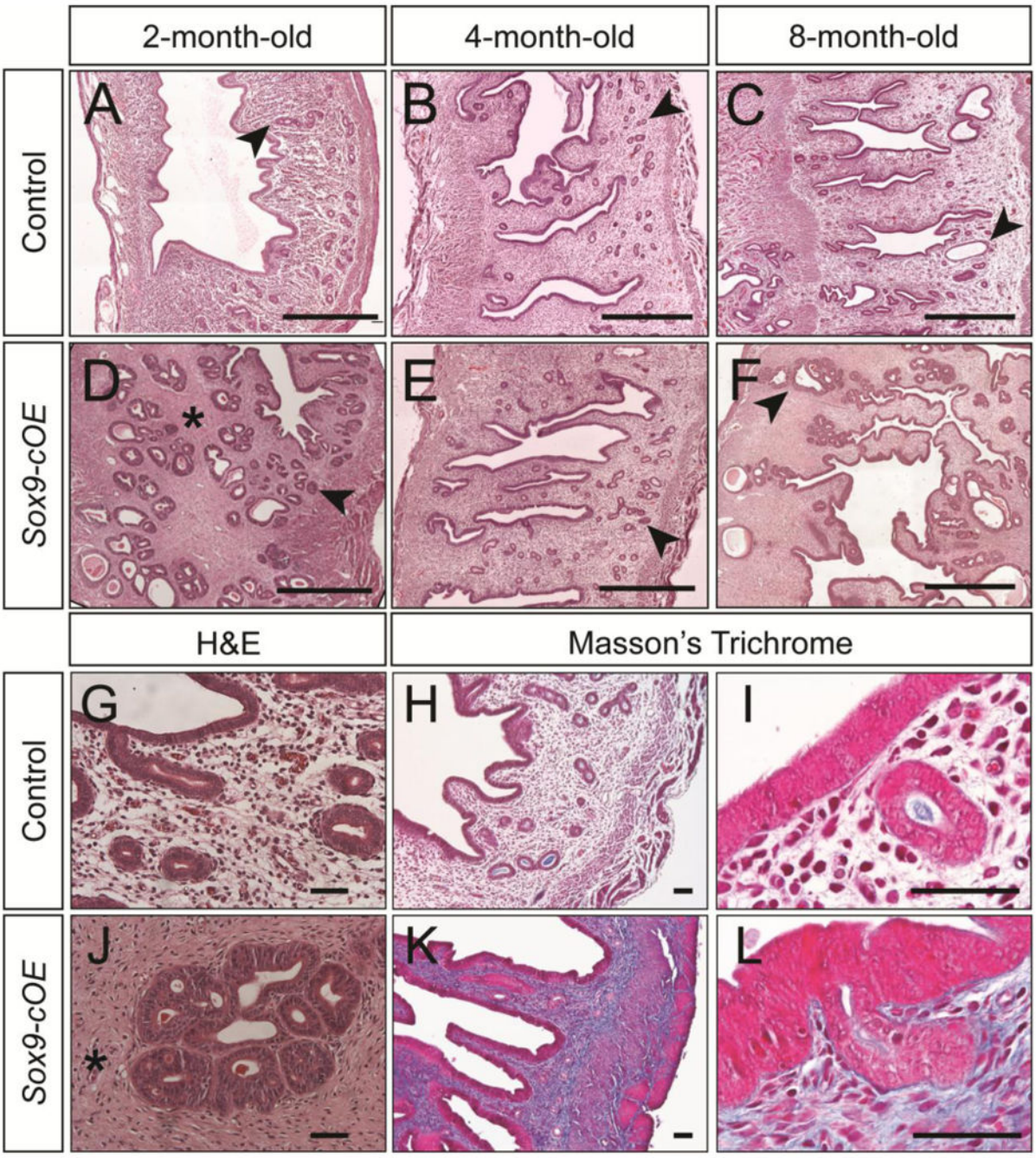

Fig. 4.

Histological analysis of Sox9-OE uteri. (A-F) H&E stained uterine sections from control (A-C) and Sox9-cOE (D-F) females at 2-, 4-, and 8-months of age. (D-F) The stroma of Sox9-cOE uteri appeared denser (asterisk) and contained dilated cystic uterine glands (arrowheads). Scale bar, 500 μm. (G, J) High magnification image of H&E stained uterine sections from 8-month-old females showing fibrotic stroma (asterisk) in Sox9-cOE females (J, asterisk). (H, I, K, L) Masson's Trichrome stained uterine sections from control (H, I) and Sox9-cOE (K, L) females at 4-months of age. More intense blue staining in the Sox9-cOE

uterine sections compared to controls indicates an increase in connective tissue/collagen fibers. (I, L) Scale bar, 50 μm. GE, glandular epithelium.

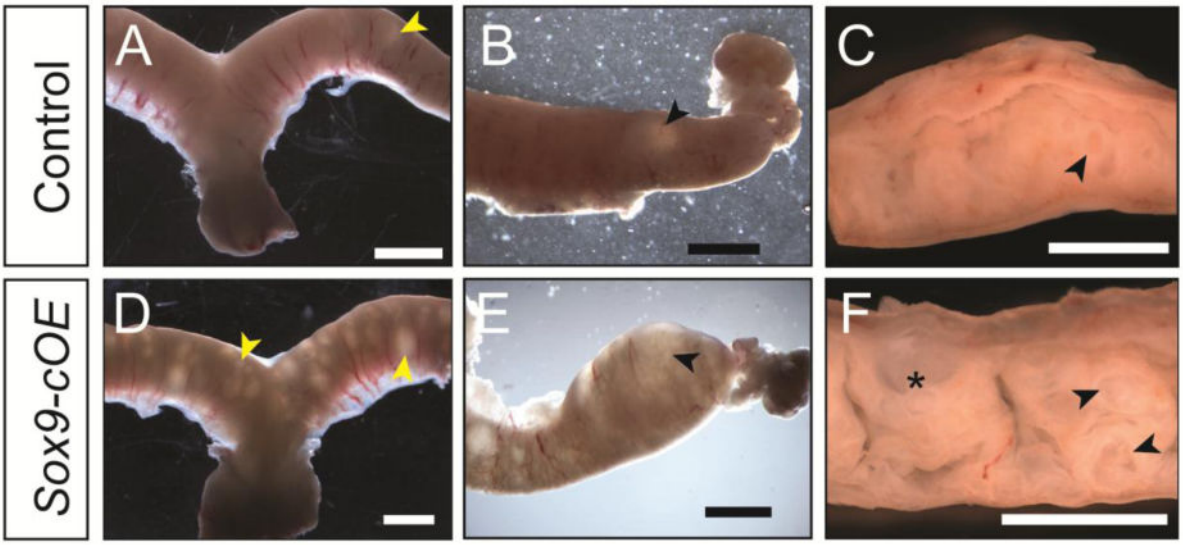

Fig. 5.

Gross morphology of 1-year old Sox9-OE uteri. (A-F) Brightfield images of 1-year-old uteri. (A-C) controls, (D-F) Sox9-cOE. (C, F) Uteri cut longitudinally (mesometrial side at the top). (A-C) 1-2 cystic structures are observed in the control uteri (arrowheads). (D-F) Numerous cystic structures (arrowheads) are present inside the uteri of Sox9-cOE females, some appeared filled with white debris (asterisk). Scale bar, 2 mm.

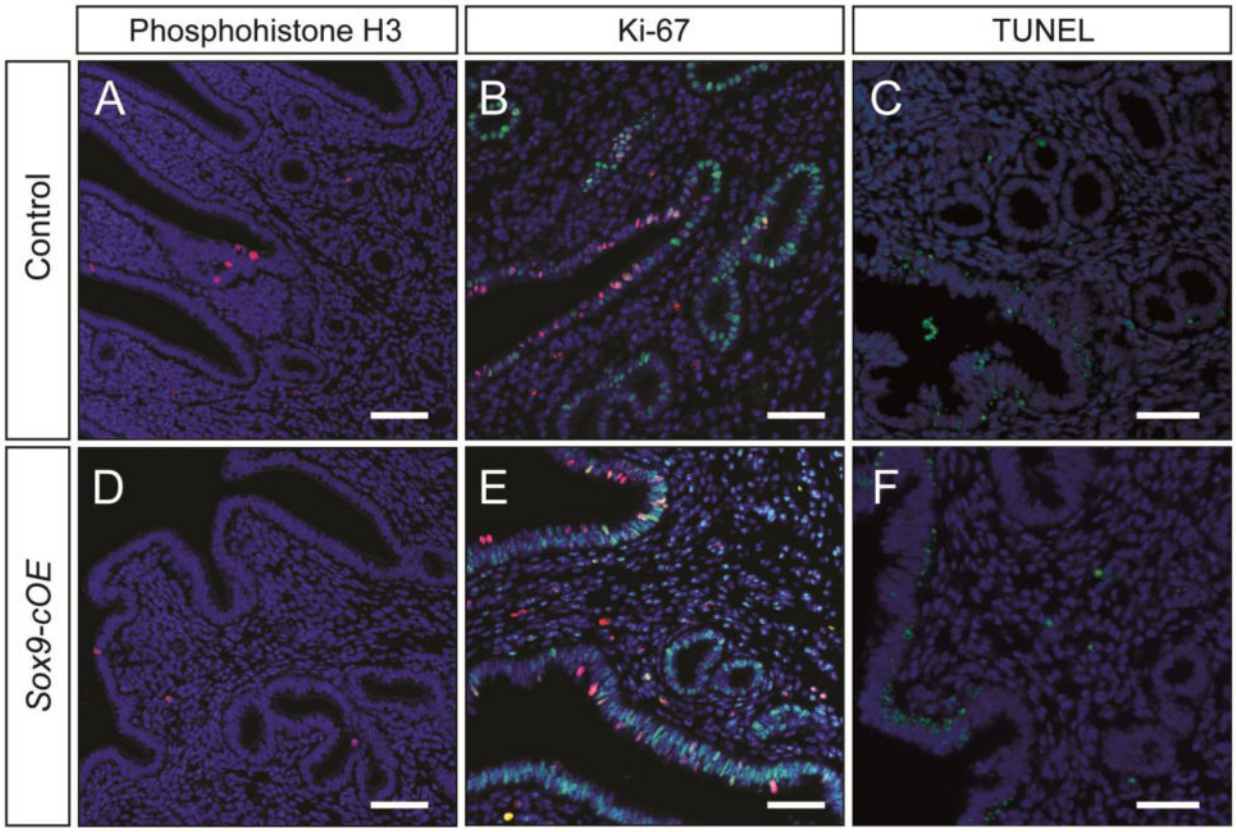

Fig. 6.

Cell proliferation and cell death analysis in Sox9-OE uteri. (A-C) Control and (D-F) Sox9-cOE 4-month-old uteri. (A, D) Immunofluorescent staining for phosphohistone H3 (red) on uterine sections taken during estrus. (B, E) Immunofluorescent staining for SOX9 (green) and Ki-67 (red) on uterine sections taken during estrus. DAPI, blue. (C, F) TUNEL assay on uterine sections taken during metestrus. TUNEL positive cells (green), DAPI (blue). Scale bar, 50 μm.

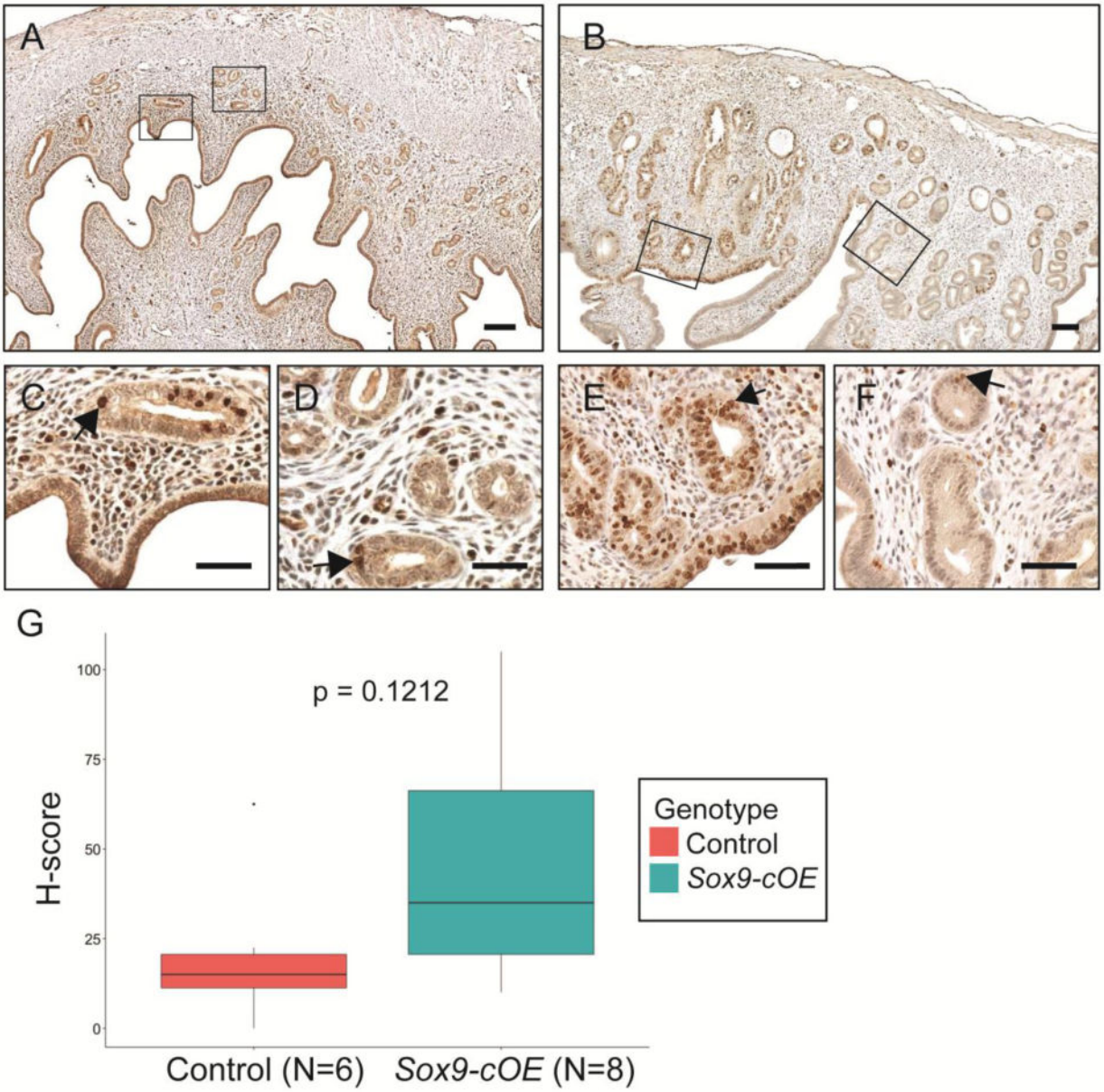

Fig. 7.

Ki-67 analysis of cell proliferation in aged females. (A-F) Immunohistochemical staining for Ki-67. (A, C, D) Control and (B, E, F) Sox9-cOE 8-month-old uteri. (C, D) Representative areas of A. (E, F) Representative areas of B to show local difference in Ki67 staining in one uterus. (G) Boxplot of H-Score analysis with standard error of the mean of 4 control and 6 Sox9-cOE uteri obtained from age-matched females. Scale bar, 100 μm.

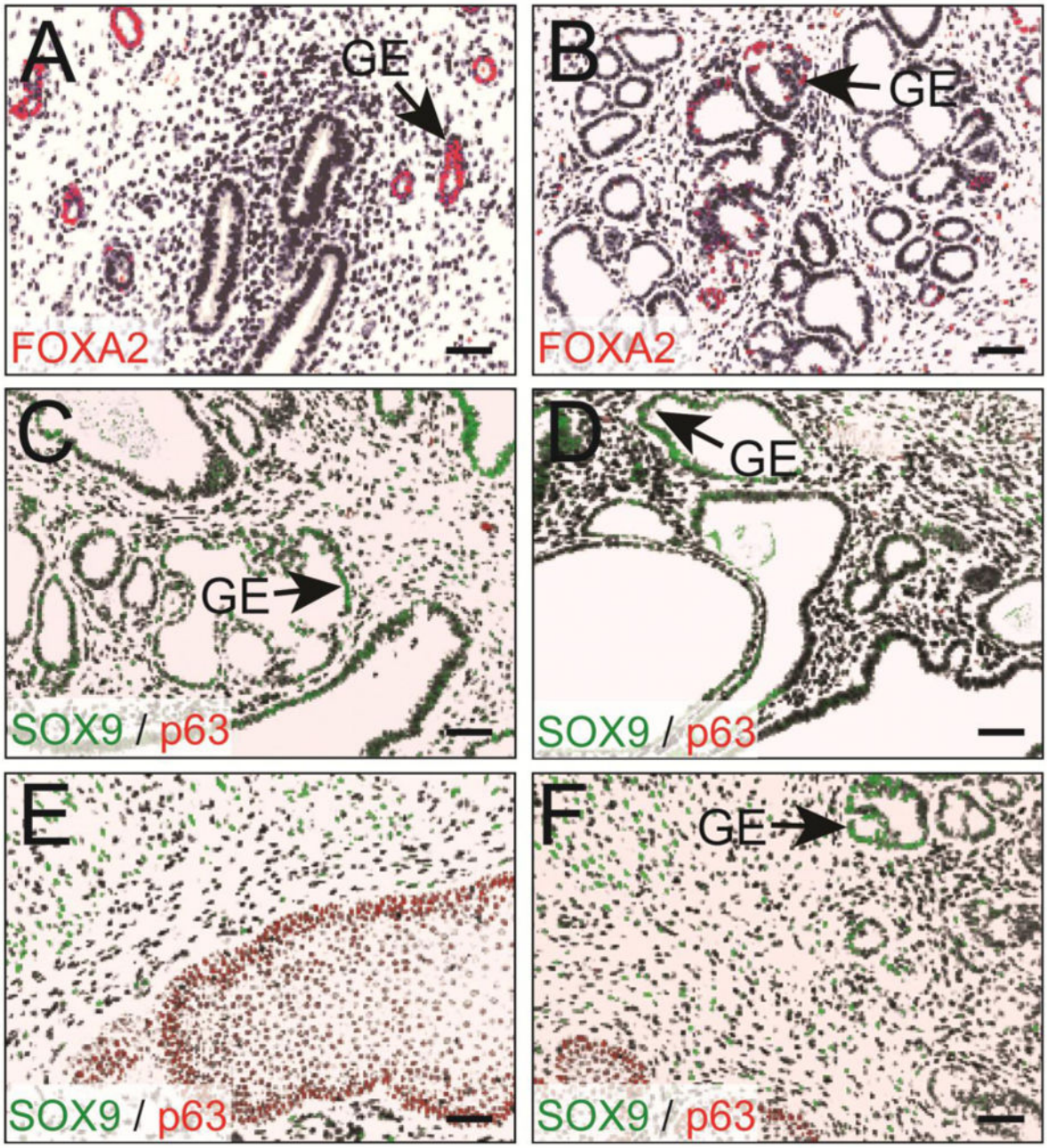

Fig. 8.

Differentiation of Sox9-OE uterine glands. Immunofluorescent staining of the uterus for FOXA2 (red), in 8-month old control (A) and Sox9-OE (B) females. (B) Cribriform uterine glands in the Sox9-OE females showed less FOXA2 immunostaining. DAPI, blue. (C-F) Immunofluorescent staining of the uterus containing dilated cystic uterine glands for p63 (red) and SOX9 (green) in 1-year-old Sox9-OE female. (E, F) Sections from 1-year-old Sox9-cOE females containing cervical epithelium. DAPI, black. Scale bar, 50 μm.